Unsaturated flow and transport through a fault embedded in fractured welded tuff

Rohit Salve, Hui-Hai Liu, Paul Cook, and Atlantis Czarnomski
Earth Sciences Division, Lawrence Berkeley National Laboratory, Berkeley, California, USA

Qinhong Hu
Lawrence Livermore National Laboratory, Livermore, California, USA

David Hudson
U.S. Geological Survey, Las Vegas, Nevada, USA

Received 7 August 2003; revised 17 February 2004; accepted 24 February 2004; published 21 April 2004.

[1] To evaluate the importance of matrix diffusion as a mechanism for retarding radionuclide transport in the vicinity of a fault located in unsaturated fractured rock, we carried out an in situ field experiment in the Exploratory Studies Facility at Yucca Mountain, Nevada. This experiment involved the release of ~82,000 L of water over a period of 17 months directly into a near-vertical fault under both constant positive head (at ~0.04 m) and decreasing fluxes. A mix of conservative tracers (pentafluorobenzoic acid (PFBA) and bromide (applied in the form of lithium bromide)) was released along the fault over a period of 9 days, 7 months after the start of water release along the fault. As water was released into the fault, seepage rates were monitored in a large cavity excavated below the test bed. After the release of tracers, seepage water was continuously collected from three locations and analyzed for the injected tracers. Observations of bromide concentrations in seepage water during the early stages of the experiment and bromide and PFBA concentrations in the seepage water indicate the significant effects of matrix diffusion on transport through a fault embedded in fractured, welded rock. *INDEX TERMS:* 1829 Hydrology: Groundwater hydrology; 1875 Hydrology: Unsaturated zone; 1894 Hydrology: Instruments and techniques; 1832 Hydrology: Groundwater transport; *KEYWORDS:* fault, flow, transport

Citation: Salve, R., H.-H. Liu, P. Cook, A. Czarnomski, Q. Hu, and D. Hudson (2004), Unsaturated flow and transport through a fault embedded in fractured welded tuff, *Water Resour. Res.*, *40*, W04210, doi:10.1029/2003WR002571.

1. Introduction

[2] An understanding of flow and transport in unsaturated fractured rock (i.e., matrix and fracture flow, and fracture-matrix interactions) is of interest in locations where there is environmental contamination or the potential for disposal of radioactive waste. These include the unsaturated fractured basalts of the Idaho National Engineering and Environmental Laboratory [*Lodman et al.*, 1994], the waste disposal facility in unsaturated chalk in the Negev desert, Israel [*Native et al.*, 1995], and the proposed radioactive waste repository in the tuff formations at Yucca Mountain, Nevada. A key factor for evaluating the performance and design of the proposed repository at Yucca Mountain is the transport of radionuclides through unsaturated fractured rock that lies between the repository horizon and water table located ~300 m below. Of particular importance is the need for an understanding of diffusive mass transfer between high-permeability, advection-dominated domains and low-permeability domains.

[3] Field investigations and numerical studies of Yucca Mountain have been conducted over the last 20 years to develop a better understanding of flow and transport. These studies have broadly suggested that the hydrology of the unsaturated zone is complicated by the complexity of fracture-matrix interactions, the nonlinearity of unsaturated flow, and the heterogenities in the hydrological properties of the fractures and the surrounding matrix. Recent conceptual models suggest that faults are possible conduits for fast flow in future climatic conditions that include an increase in precipitation [e.g., *Bodvarsson et al.*, 1999].

[4] Within the last three decades, there has been an increased appreciation for the importance of matrix diffusion in the subsurface transport of solutes [e.g., *Neretnieks*, 1980; *Maloszewski and Zuber*, 1993] (see also the work of *Wood* [1996] as reported by *Meigs and Beauheim* [2001]). However, while several field studies have investigated matrix diffusion processes in saturated fractured rock [e.g., *Albelin et al.*, 1991; *Novakowski and Lapcevic*, 1994; *Hadermann and Heer*, 1996; *Jardine et al.*, 1999; *Callahan et al.*, 2000; *Shapiro*, 2001; *Reimus et al.*, 2003], very few field studies have investigated these processes in unsaturated fractured rock environments [e.g., *Hu et al.*, 2001].

[5] Laboratory studies of diffusion in fractured matrix have also been limited to saturated conditions, mainly due

to the relative simplicity of experimental systems and result interpretation, and the interest in contamination and remediation of aquifer systems. In saturated volcanic tuff, *Callahan et al.* [2000] confirmed the importance of matrix diffusion in increasing the transport time of solutes, by spreading mass away from the advective region of the fractures. On the other hand, numerous articles have been published about aqueous solute diffusion in unsaturated geological media, including unconsolidated and aggregated media, as reviewed by *Hu and Wang* [2003].

[6] The influence of matrix diffusion under unsaturated conditions can be evaluated in field experiments by introducing multiple tracers, with distinct coefficients of diffusion, into a fractured rock flow regime. The collected samples are then analyzed to determine the pattern of tracer breakthrough. For this purpose, the collected samples of seepage must span the duration of tracer migration through the test bed, and the sampling frequency must be optimized to capture temporal changes in tracer concentrations. However, it is difficult to obtain a complete sample record of subsurface experiments in unsaturated fractured rock, because neither the location of seeps nor the start, rates, and duration of flow can be known a priori. This limitation has mandated the development of new techniques for sampling tracer-laced seepage during field experiments.

[7] This paper presents the results of a field investigation, the broad objective of which was to study unsaturated flow and transport through a 20 m vertical section of fault located in the fractured welded tuff of the Topopah Spring Tuff unit (TSw) at Yucca Mountain, Nevada. Specifically, the goal was to evaluate the importance of matrix diffusion as a mechanism for retarding radionuclide transport in the vicinity of a fault located in unsaturated fractured rock. Included in this paper are techniques developed to conduct the in situ field experiment, observations of seepage, and tracer transport as water released along the fault traveled the ~20 m vertical distance through the test bed. The remaining sections of this paper include a discussion on important implications derived from these test observations.

2. Methods

[8] Water was released along a horizontal section of the fault under ponded conditions over a period of thirteen months, and then under reduced fluxes for another six months. When quasi-steady state seepage was observed at the lower end of the test bed, two tracers with different molecular diffusion coefficients were introduced into the ponded water infiltrating the fault. After tracer-laced water had been released into the fault, more tracer-free water was released, and seepage from three locations along the fault was analyzed for the presence of the two tracers.

2.1. Test Bed

[9] The test bed for this study was located in the Exploratory Studies Facility (ESF), an underground research laboratory at Yucca Mountain, ~120 km north of Las Vegas, Nevada. The ESF includes a 8 km long, 8 m diameter tunnel, the Main Drift, which was excavated in 1996, and a second 3 km long, 5 m diameter tunnel, the Cross Drift (Figure 1a). The Cross Drift was excavated in 1998 as a branch from the Main Drift, such that it crosses over the Main Drift at a vertical distance of ~20 m.

[10] The test bed study extends from ~190 to ~210 m below ground surface, with the upper and lower boundaries defined by the Cross Drift and the Main Drift, respectively (Figure 1b). To facilitate controlled releases of water and monitoring of seepage, two cavities were excavated horizontally into the walls of the Cross Drift and Main Drift. The cavity excavated in the Cross Drift, referred to as alcove 8, is approximately 30 m long by 6 m wide. Niche 3, which is the cavity excavated in the Main Drift, is separated from alcove 8 by a vertical distance of ~20 m, is 4 m wide, and extends ~14 m from the centerline in the Main Drift. alcove 8 is located within the Topopah Spring Tuff upper lithophysal zone (Tptpul). Niche 3, which lies vertically below alcove 8, is located within the Topopah Spring Tuff middle nonlithophysal zone (Tptpmn) (stratigraphic nomenclature of *Buesch et al.* [1996].

[11] The focus of this study was a near-vertical fault that cuts across the test bed in alcove 8. Within the alcove, the fault is open along the sides and ceiling, with an aperture of 0.01–0.02 m, and appears to be sealed with infill along the floor. The fault is visible along the ceiling of niche 3, vertically below the trace along the floor in alcove 8. Because of the large degree of fracturing along the ceiling of niche 3, and the location of a bulkhead at the entrance of the niche, it is difficult to provide an estimate of the width of fault aperture. In the formation between alcove 8 and niche 3, we do not have a reliable method by which to assess the width of the fault and also the extent to which the infill material is present.

2.2. Liquid Release

[12] Water was released along a 5.15 m section of fault visible on the floor of alcove 8 (Figure 2a). The section of fault visible along the floor of alcove 8 was chiseled to create a trench to facilitate the ponded release of water along the fault section. This trench was partitioned into four sections with steel plates, with each section serving as a separate release point. Along sections 1–3, the width of the trench ranged between 0.43 and 0.46 m. In section 4, the trench was excavated to include a square with 2.05 m of fault running through it diagonally. Each section had a permeameter for water application measurement; all four permeameters were supplied by a single water tank (Figure 2b). The permeameters were designed to maintain the desired height of ponded water (i.e., ~0.04 m), while continuously monitoring the rate at which water was released into the infiltration zone. Under ponded conditions, the wetted area for the first three sections was 0.40, 0.47, and 0.53 m^2, respectively. In the fourth section, the wetted area was significantly larger (2.1 m^2) because of the length of fault and also because of the extended boundaries of the trench.

[13] Between 6 March 2001 and 8 April 2002, ~76,000 L of water were released into the fault under ponded conditions (i.e., a head of ~0.04 m). In the ensuing six months, an additional 5000 L of water were released into the fault under a gradually decreasing flux.

2.3. Tracer Release

[14] A mix of conservative tracers (pentafluorobenzoic acid (PFBA) and bromide (applied in the form of lithium bromide)) was released along the fault seven months after the start of release of water along the fault. (The free water diffusion coefficients for bromide and PFBA are 21.5 ×

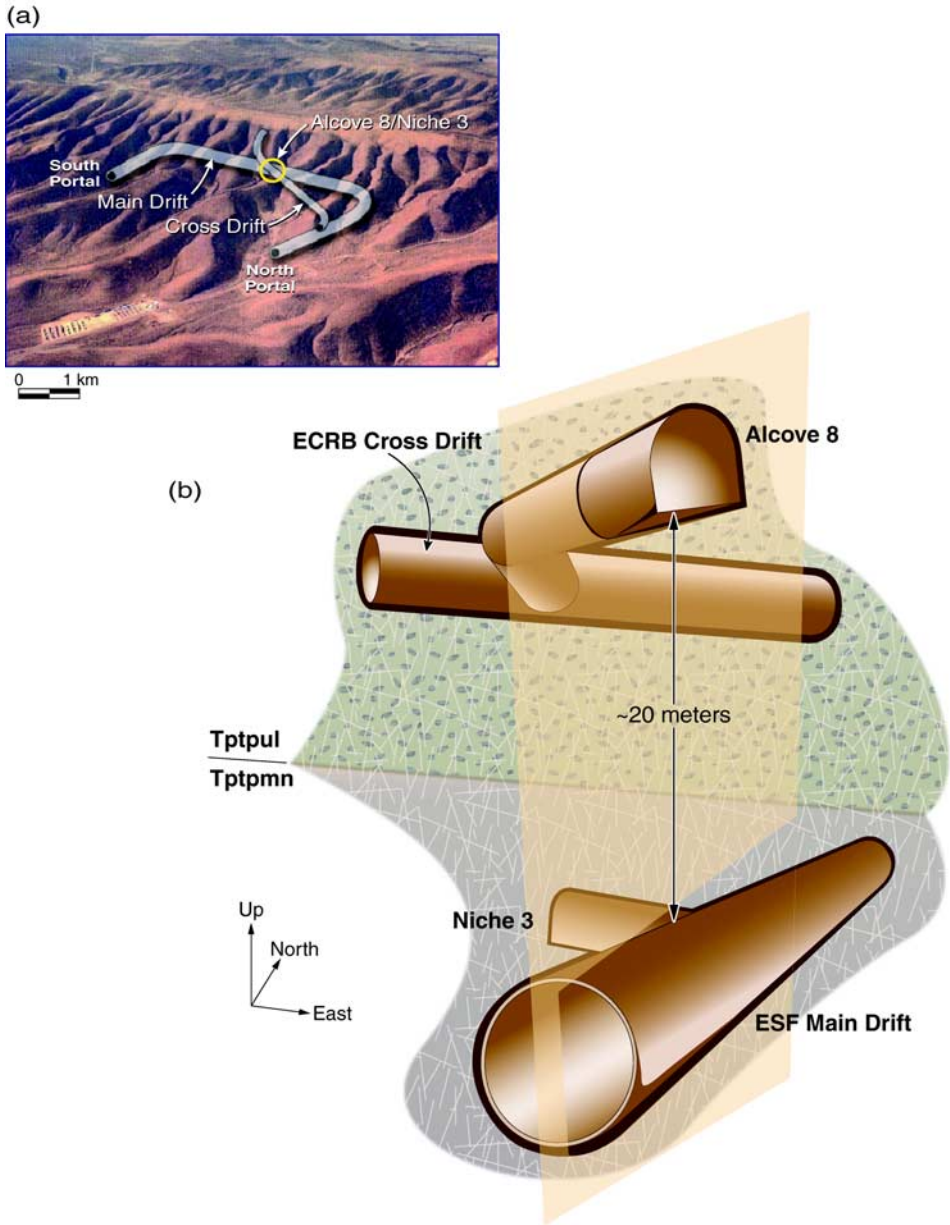

Figure 1. (a) Three-dimensional view of tunnels in the Exploratory Studies Facility at Yucca Mountain; (b) the test bed for this study (alcove 8/niche 3), located at the crossover point of the two tunnels.

10^{-10} m^2 s^{-1} and 7.6×10^{-10} m^2 s^{-1}, respectively [*Callahan et al.*, 2000]). This application, which began on 1 October 2001, after ~43,000 L of ponded water had infiltrated the fault, extended over a period of nine days. The concentration of lithium bromide in the tracer mix was ~500 mg/L, and the concentration of the injected PFBA was ~25 mg/L. These concentrations were achieved by dissolving 50 g of PFBA and 1000 g of the lithium bromide in 1893 L (500 gallons) of water. Note that these tracers were in addition to lithium bromide (20–30 mg/L) included in all water introduced into the ESF for mining-related activities and for most scientific investigations.

2.4. Seepage Monitoring

[15] Water percolating through the fault from alcove 8 and seeping into niche 3 was collected in plastic trays and diverted to PVC collection bottles. The ceiling of niche 3 was blanketed with an array of trays to capture seepage. Seepage rates were continuously monitored with an automated, remotely accessed water collection system connected to the trays.

[16] A schematic of the seepage collection system is shown in Figure 3. The key components of this system included collection bottles, air-activated pinch valves, pressure transducers, and a control and recording system. Each collection bottle was 1.5 m tall, 20 cm in diameter, and had three ports, one at the top and two at the bottom. The port at the top served as the inlet to the bottle and was connected to a pinch valve. One of the ports at the bottom served as the outlet to the bottle and was also connected to a pinch valve. A differential pressure transducer was connected to the third port.

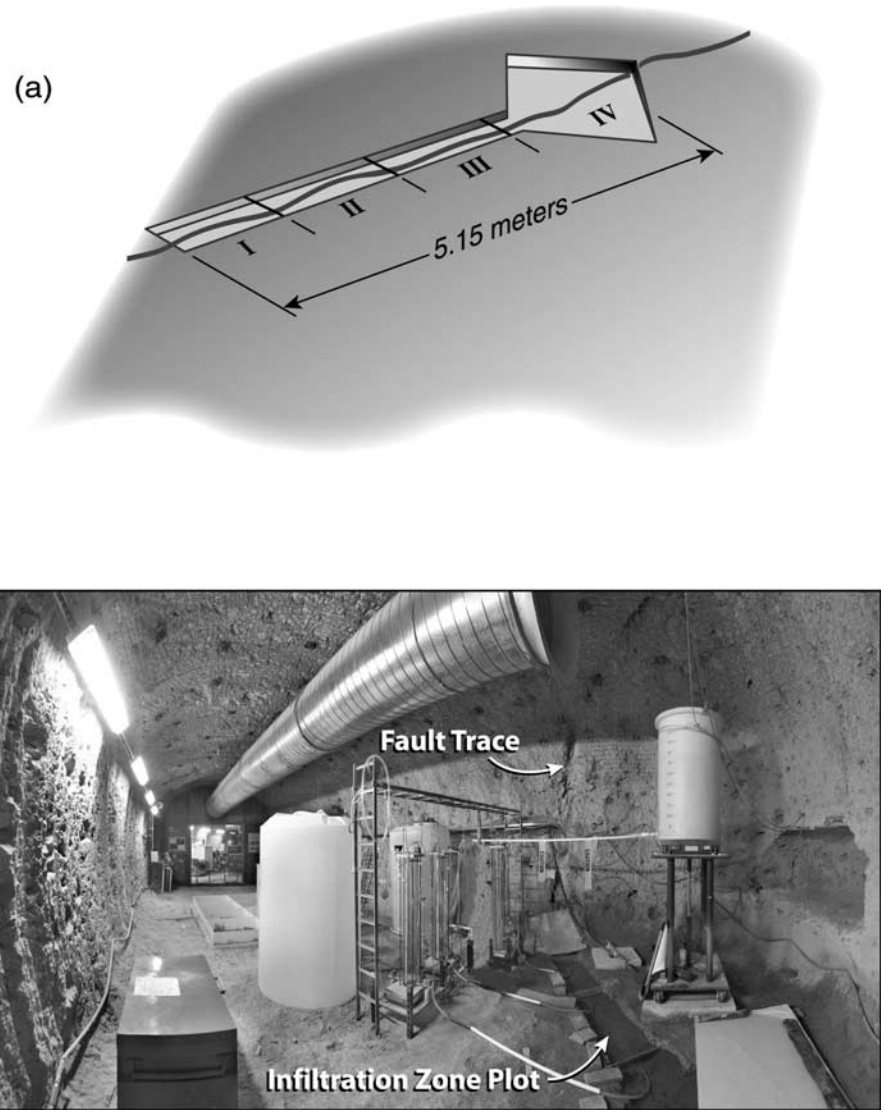

Figure 2. (a) Schematic of the fault zone in alcove 8 into which water and tracers were released; (b) photograph of alcove 8 showing the fault covered with ponded water and the permeameters and tanks used to supply water to the fault zone.

[17] When water began to seep into an initially empty bottle, the pinch valve at the top remained open while the valve at the bottom was closed. This configuration was maintained until water in the bottle reached a predetermined height. To purge the bottle, the pinch valve at the top was closed and the valve at the bottom was opened. Once the bottle was drained, the valves were reconfigured to fill the bottle. The pinch values were pneumatically actuated via air lines controlled by solenoids. Computer-controlled electronic relays operated the solenoids. Voltage signals delivered by an analog-to-digital converter with a multiplexer converted the transducers' current loop output to digital format, which was recorded by the same computer used for valve control.

[18] The computer system for the water collection system continuously recorded the transducer outputs and enabled the seepage collection process to be manually or automatically controlled. The computer system also incorporated a remote control capability, so that the system could be started and controlled from any networked computer.

2.5. Tracer Sampling

[19] Because of the inaccessibility of the test bed for long durations, a tracer sampling system, the passive-discrete water sampler (PDWS), was developed that could automatically collect continuous samples of water [*Salve*, 2004]. Here the main design concern was the development of a single tool that could be deployed and left largely unattended over extended periods (days to weeks) to (1) measure seepage rates and (2) isolate discrete samples of water (for chemical analysis) seeping from the ceiling of niche 3. This was achieved by attaching a series of sampling bottles along a vertical stem, the lower end of which terminated into a differential pressure transducer (Figure 4a).

[20] After seepage enters the PDWS at the top of the stem, it travels vertically downward to the bottom of the

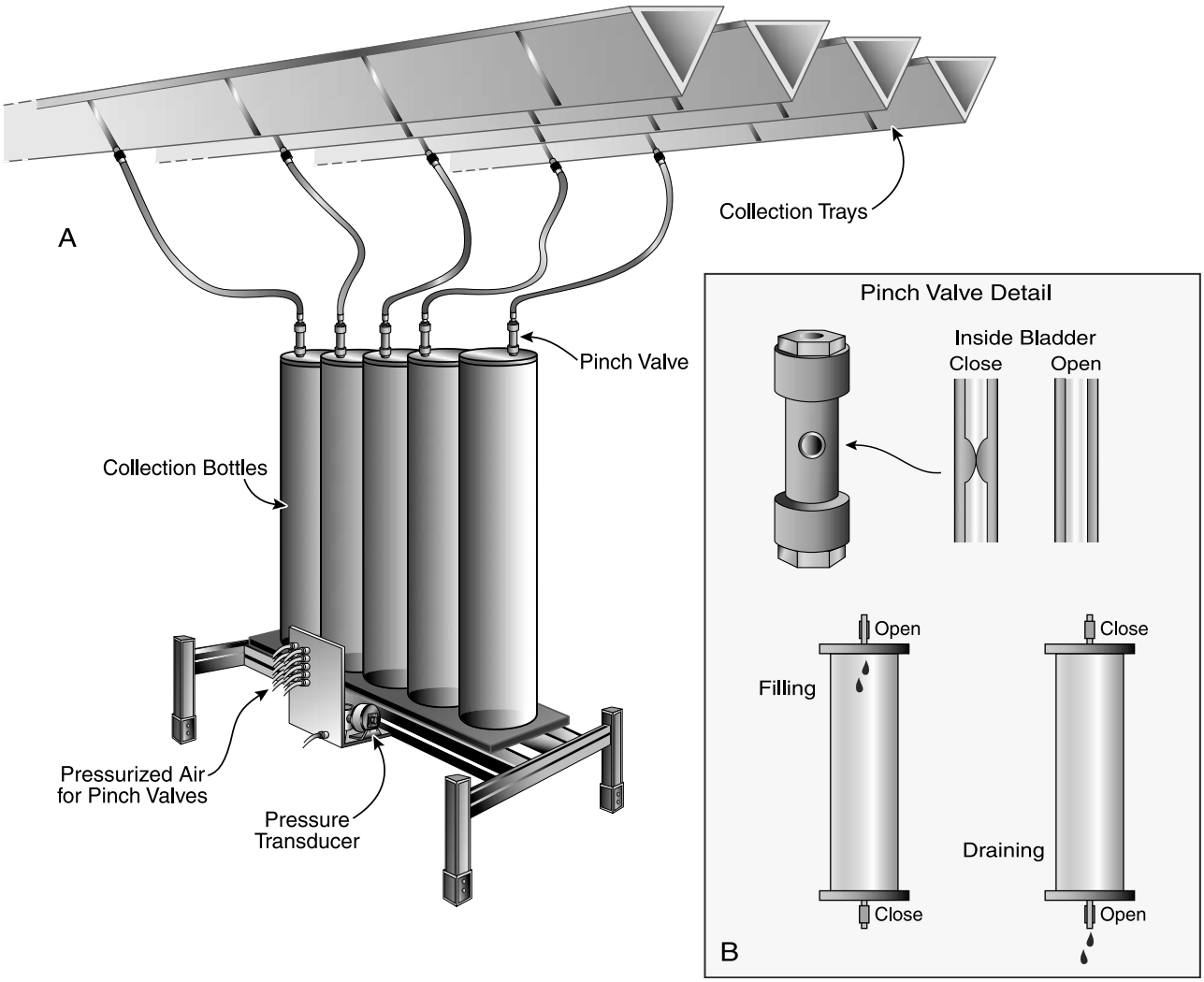

Figure 3. (a) Schematic of the automated seepage monitoring system; (b) insert showing how the pinch valves monitor the filling and draining of seepage collection bottles.

stem. As more water collects, the stem begins to fill, and water rises to the inlet of the lowest bottle, from where it is diverted into the first sample bottle. After the first bottle is filled, additional water fills the vertical stem until the water reaches the inlet to the second bottle, and so on, until all bottles along the stem are filled. If a large number of samples is to be collected from a single location, an appropriate number of vertical stems can be connected in series such that after bottles along a single stem are filled, additional water is transferred to an adjacent stem.

[21] The pressure transducer, which records (as head) the height of water at any given moment along the length of the vertical stem, is connected to a programmable data logger such that the frequency of measurements can be controlled. Seepage rates during the collection of a particular sample can be determined from the sample volume and the time at which the sample (constant pressure) was collected.

[22] Water was collected from three seepage locations for analysis of tracer concentrations (Figure 4b). These included the point where the first seeps were observed on 6 April 2001 (tray 6), in niche 3 following the release of water along the fault. The other two collections points were tray 7, where seepage rates were relatively low during the period immediately before the release of tracers, and tray 9 + 23, where the seepage rates where the highest among all the locations at which seepage was observed. (The two trays 9 and 23 were lumped into one collection point because of the limited collection bottles that were available to collect the seepage.)

[23] All three sampling locations were along the trace of the fault in niche 3. As the application of tracers began in early October 2001, water seeping into three trays in niche 3 (i.e., tray 6, tray 7 and tray 9 + 23) was diverted to three individual PDWS units. Over the next three months, the trays remained connected to the PDWS, and water samples collected from these units were analyzed for concentrations of the introduced tracers.

3. Observations

3.1. Seepage in Niche 3 Under Ponded Conditions

[24] During the first two months of ponded release, large disruptions to the daily application rate occurred as ~15,000 L of water were applied along the fault. Once the supply of water was stabilized, varability in infiltriation rates decreased, and the rate at which water moved into the fault gradually decreased as well. During the period be-

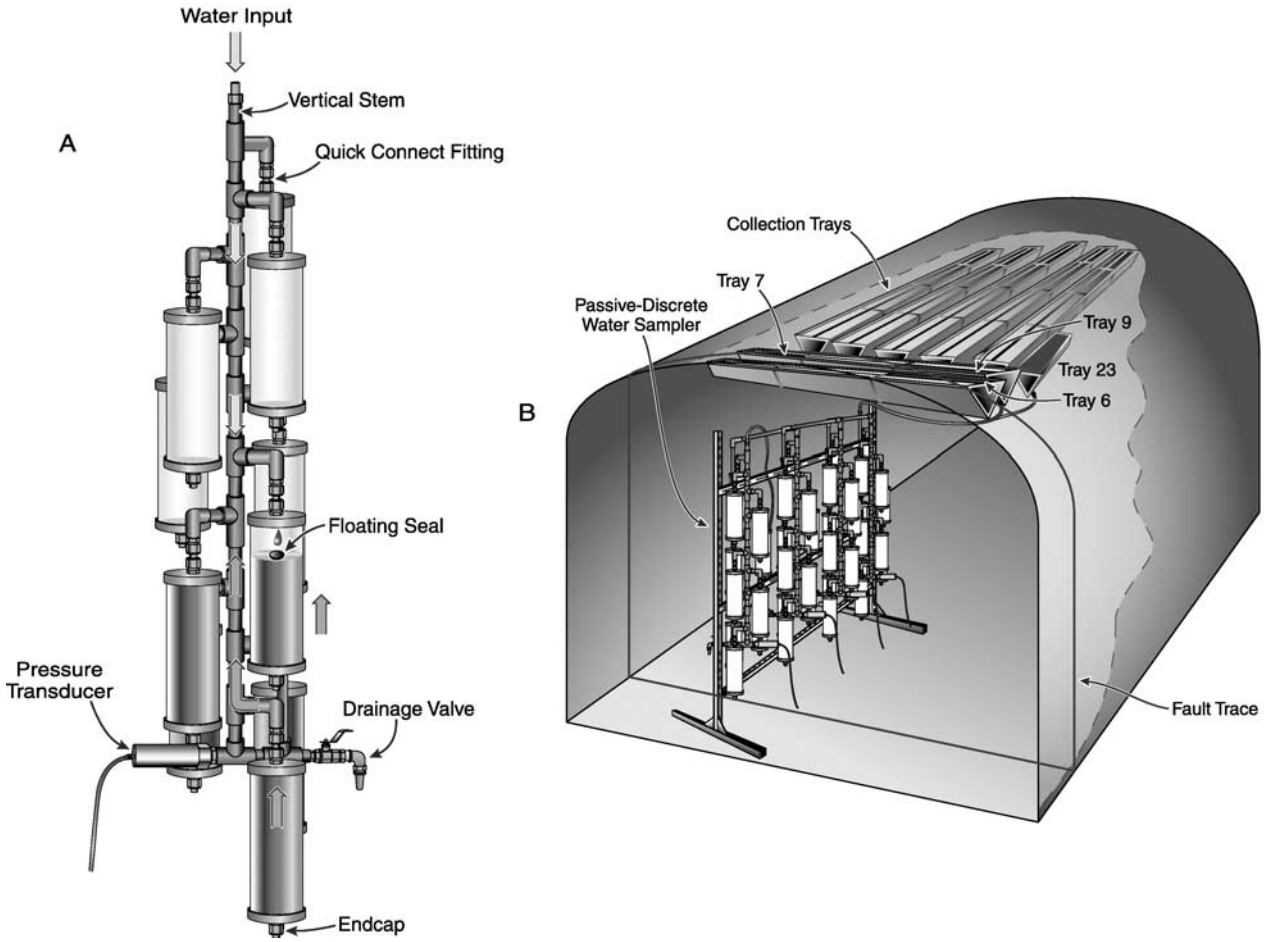

Figure 4. (a) Schematic showing design and components of the passive-discrete water sampler; (b) location of tray 6, tray 7, and tray 9 + 23, from which seepage was collected for analysis of tracer concentrations.

tween late April 2001 and early October 2001, just before tracer application to the fault, the infiltration rate fell from ~300 L/day to ~210 L/day (Figure 5). Thirty-one days after the start of water release, the wetting front was first detected ~19 m vertically below along a borehole intersecting the fault 1 m above the ceiling of niche 3 (R. Salve et al., Development of a wet plume following liquid release along a fault, submitted to *Water Resources Research*, 2003) (hereinafter referred to as Salve et al., submitted manuscript, 2003). Drips of water were first observed along the fault at niche 3 on 10 April 2001, 35 days after the initial release of water along the fault. Over the next few weeks, the number of seeps along the fault gradually increased, and the seepage rate within niche 3 increased to 25 L/day by late April 2001, before gradually decreasing over two distinct periods to 15 L/day by early October 2001 (Figure 5).

[25] Measurable seepage was observed in 10 locations close to the fault trace along the ceiling of niche 3. Further into the niche, the ceiling was visibly damp (though not dripping) up to a distance of 2–3 m from the fault trace. The first seeps were observed above tray 6, where seepage rates climbed rapidly to ~8 L/day over a period of two weeks, before dropping sharply to rates below 2 L/day by early August 2001 (Figure 6). A similar temporal pattern was observed from tray 9 + 23, where seepage rates reached ~9 L/day over a period of 2–3 weeks before steadily decreasing to ~3 L/day by late January 2002. The most consistent seepage rates (i.e., between ~ 3–6 L/day) were maintained at tray 8. At other locations along the niche ceiling, seeps were observed significantly later. At these locations, seepage was sporadic and occurred at rates that were consistently less than 3 L/day.

[26] The amount of water recovered as seepage varied significantly during the 13 months that seepage was observed in niche 3 (Figure 7). There was an initial period between mid-April and mid-May 2001 when the percentage of injected water that was recovered sharply increased to ~8%. Over the next 5 months (until the start of tracer releases), the recovery percentage fluctuated between 5 and 11%. After tracer sampling was completed and constant head release was replaced by a decreasing flux at the upper boundary, the recovered seepage also rapidly decreased.

3.2. Tracer Recovery in Niche 3

[27] From the time that the first seep was observed in niche 3 (on 9 April 2001), water samples were periodically

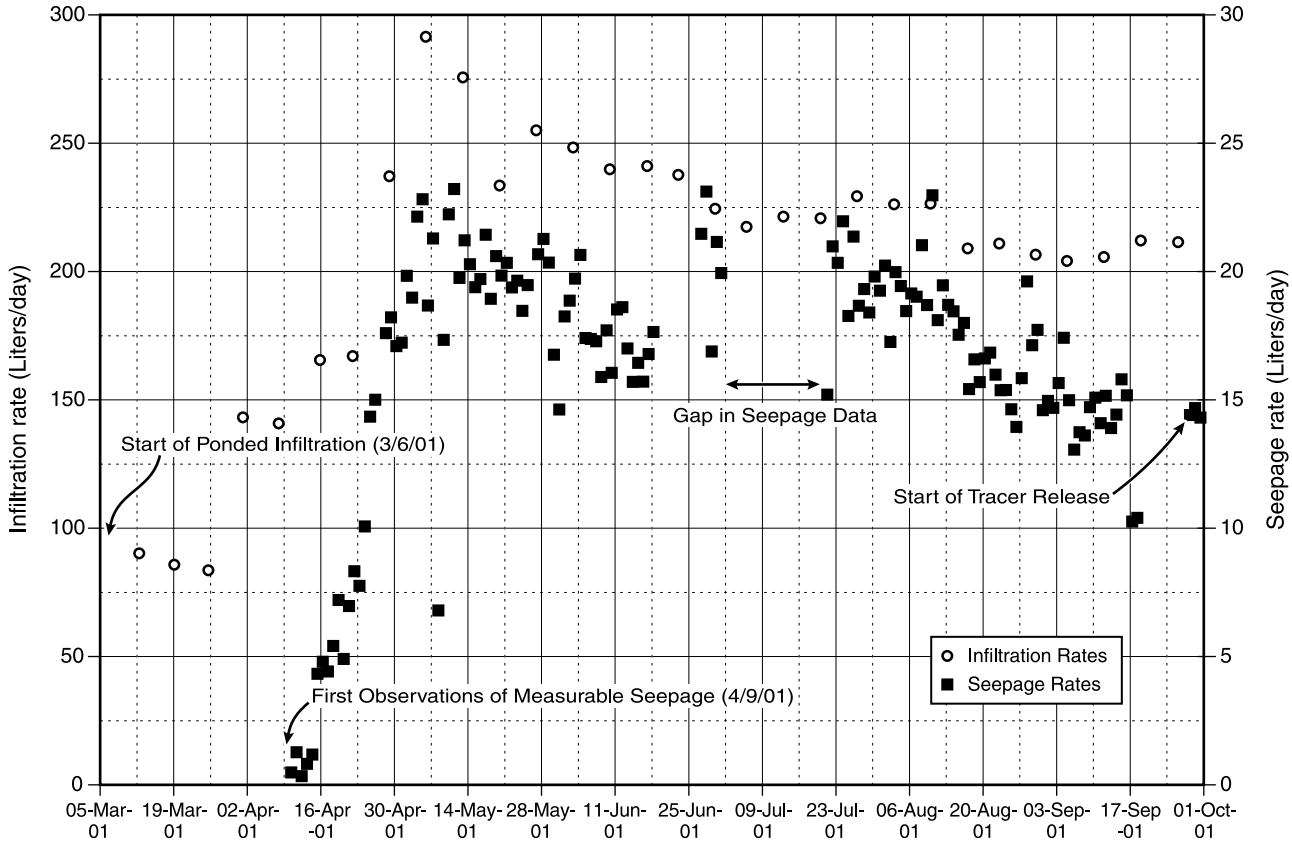

Figure 5. Infiltration and seepage rates measured in alcove 8 and niche 3, respectively, for the 7 months of ponded water release prior to the application of tracers along the fault.

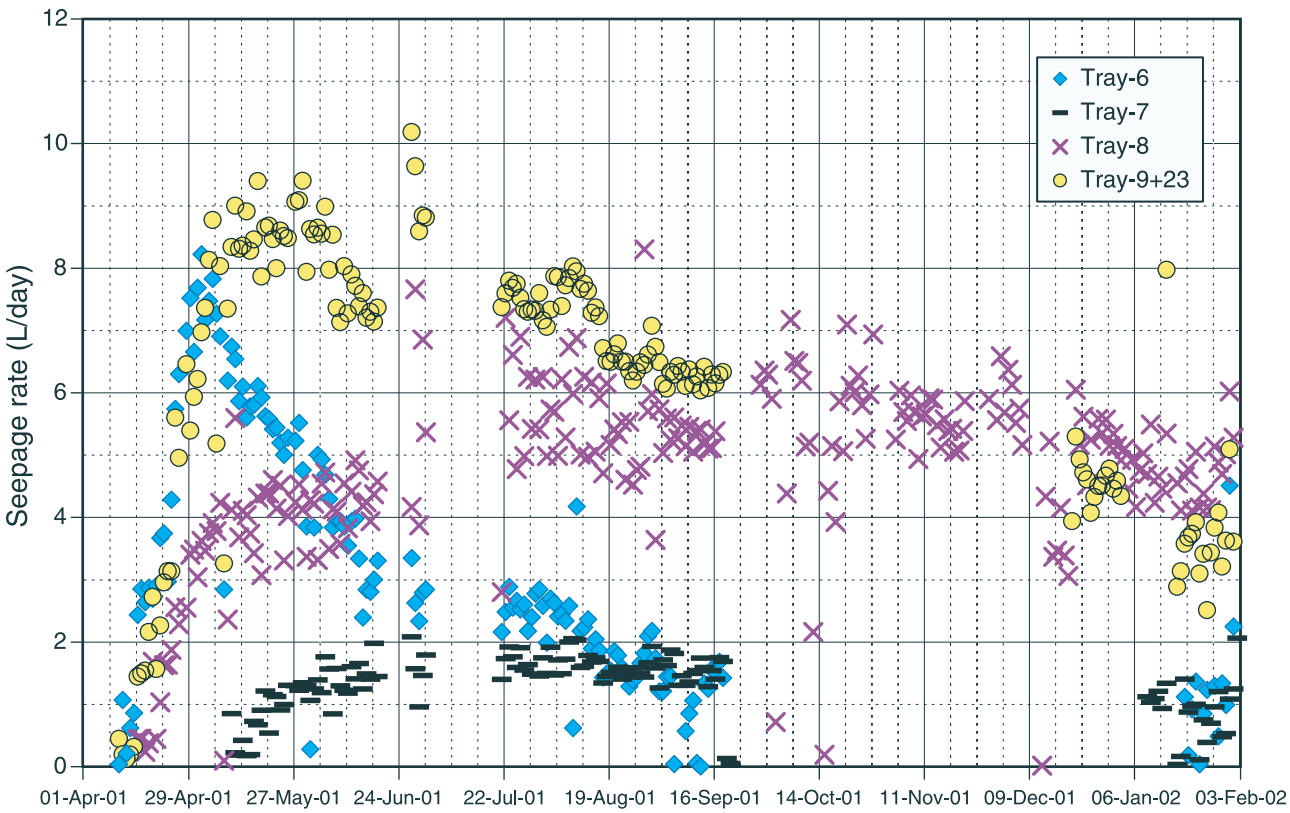

Figure 6. Seepage rates (in L/day) from four of the 10 locations where measurable seepage was observed. Note that for the three locations from which seepage was sampled for tracer concentrations (i.e., trays 6, 7, and 9 + 23), no seepage rates are presented for the duration of sampling.

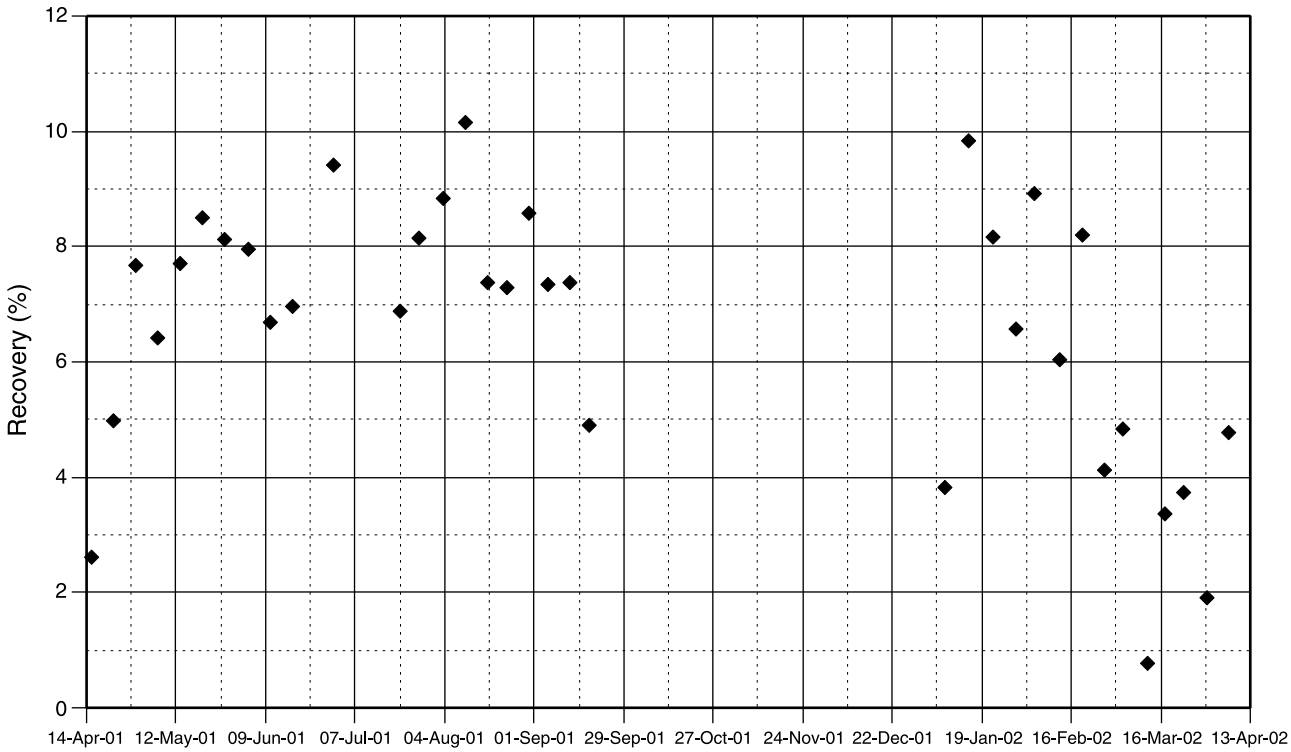

Figure 7. Percentage of injected water recovered from all the trays in niche 3 in which seepage was collected during the period when ponded water was introduced in alcove 8. Excluded is the period during which water samples were removed for tracer analysis.

collected from the location of the first seep (tray 6) and analyzed for bromide concentrations. Six months later, when the tracer mix was introduced with the infiltrating water, seepage from three locations along the niche 3 ceiling were sampled (i.e., tray 6, tray 7, and tray 9 + 23). During the period between 1 October 2001 and early January 2002, all water seeping from the three locations was collected as discrete samples and analyzed for concentrations of bromide and PFBA.

[28] Figure 8 shows the concentration of bromide measured in the seepage water from tray 6 along with the daily seepage rates for the 45-day period immediately following arrival of the wetting front. The bromide concentration was initially low (about 3 ppm), then increased gradually to a steady state plateau value of about ~25 mg/L, which is similar to that for water applied along the infiltration plot (24.8 ± 3.6 mg/L, N = 15, over a duration of 11 weeks). Note that the bromide detected is from the background

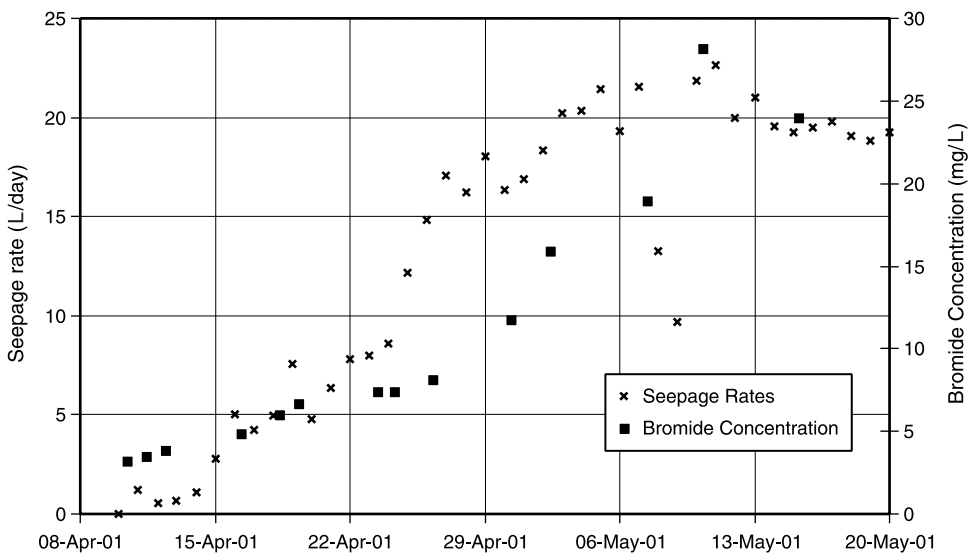

Figure 8. Concentration of bromide plotted against seepage rates measured from all trays in niche 3 in which seepage was collected, for a period of 45 days after first observations of drips in tray 6.

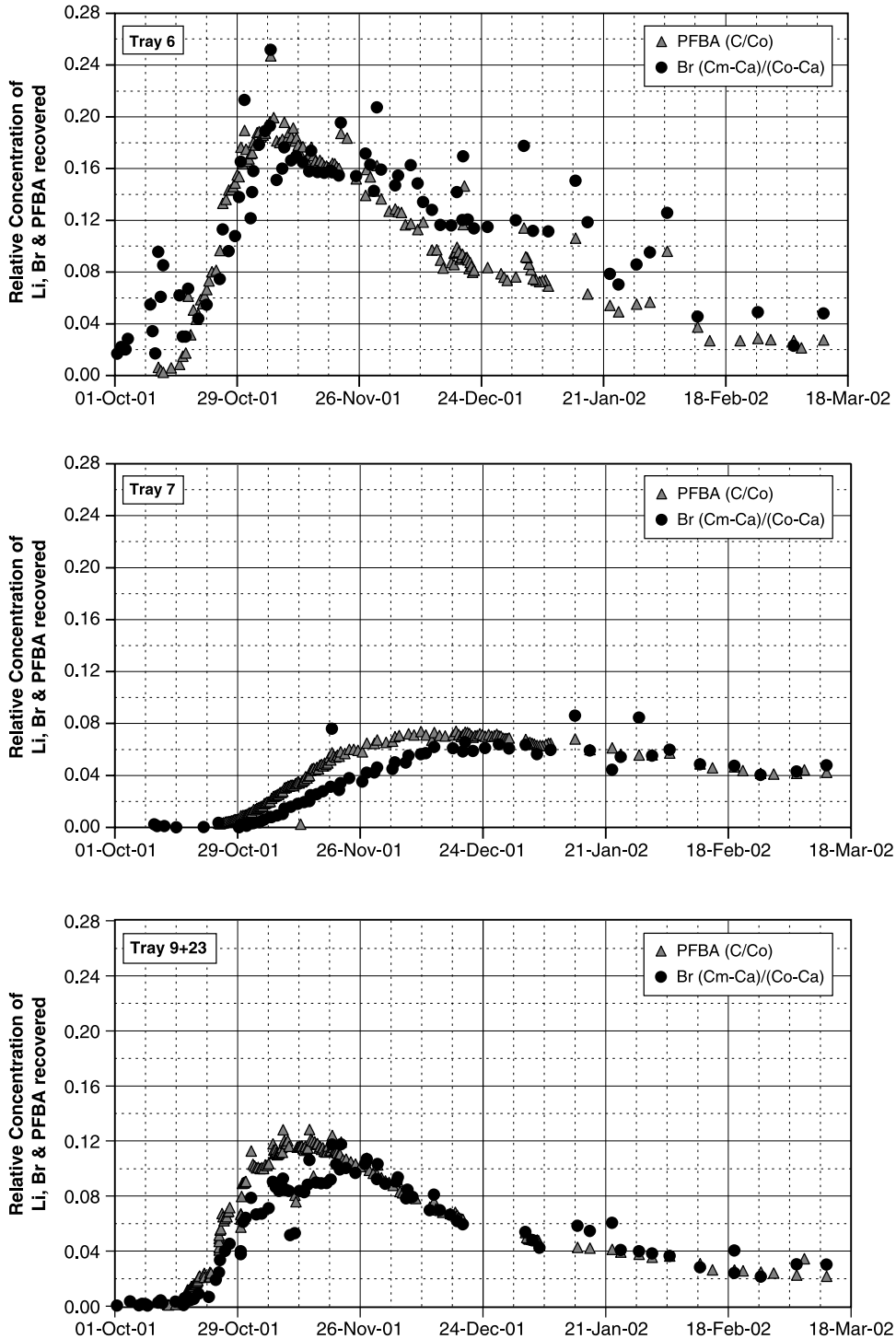

Figure 9. Concentration of bromide and PFBA measured in seepage water collected at three locations in niche 3. Tracer pulse was applied on 1 October 2001 in alcove 8 and lasted for 9 days.

concentration (prior to tracer test) in the injected water. Variability of the plateau value is related to the variable application concentration of bromide. Increasing bromide concentrations more or less paralleled seepage rates.

[29] Figure 9 presents the tracer concentration in the seepage water collected from the three sampling locations. In the three plots the concentration of bromide has been normalized (by subtraction) to account for bromide concentrations in the injected water, which contains a tagging of about 25 mg/L bromide. The first arrival and, subsequently, the largest amount of tracers recovered were in water sampled from tray 6. Here the first traces of PFBA and elevated values of bromide were detected approximately 10 days after the tracers were applied along the fault. The concentration of both bromide and PFBA continued to rise rapidly in the water sampled from this location for a period of three weeks, before gradually dropping over the next five months (though the tracer pulse was applied for a duration

of only 9 days). The peak concentrations of the tracers at this location occurred 39 days after the start of tracer release in alcove 8, suggesting a transport velocity of ~0.51 m/day. This travel time is less than that measured for the initial wetting front (i.e., 0.61 m/day) following the release of water into the fault at the start of the experiment (Salve et al., submitted manuscript, 2003). There was relatively small variability in the increasing tracer concentrations during the initial three weeks, unlike the ensuing period of sampling when the concentration of bromide and PFBA showed significant variability as the amount of tracers in the sampled water continued to decrease. Because of the large temporal variability in tracer concentrations, it was difficult to discern whether PFBA breakthrough preceded bromide at this location.

[30] In tray 7, both bromide and PFBA were first detected three weeks after initial application of the tracers along the fault. In the following month, the concentration of both the tracers gradually increased, with the PFBA concentrations clearly preceding bromide. Peak concentrations of PFBA at this location were observed 61 days after the start of tracer release in alcove 8, suggesting a transport velocity of ~0.32 m/day. Over the next three months, the concentration of both tracers gradually decreased. During the final month of sampling, the tracer concentrations remained relatively constant.

[31] In tray 9 + 23, the first arrival of bromide and PFBA was similar to that observed in tray 6. However, unlike tray 6, the temporal variability in the bromide concentrations was significantly less. Moreover, except for the period between mid-October and late November 2001 (when the PFBA concentrations suggest faster travel through the fault zone), both tracers showed a similar temporal recovery pattern. The peak concentrations of tracers at this location were observed 43 days after the start of tracer release in alcove 8, suggesting a transport velocity of ~0.46 m/day.

4. Discussion

4.1. Capillary Barrier Effect

[32] Water released along the fault in alcove 8 flowed relatively quickly along the fault and into adjacent fractures connected to the fault (Salve et al., submitted manuscript, 2003). When water arrived above the niche ceiling, it likely did not immediately seep into the niche because of potential capillary barrier effects [*Philip et al.*, 1989; *Birkholzer et al.*, 1999]. While capillary effects have been well documented for porous media, the existence of such impedance to flow in unsaturated fractured rock has not been extensively demonstrated. Most recently, the capillary barrier effect corresponding to underground openings in unsaturated fractured rock was demonstrated by *Trautz and Wang* [2002], who observed the spreading of a wetting front across the ceiling of a drift and up into fractures during liquid release tests.

[33] If existing, the capillary barrier could divert flow away from the niche ceiling, resulting in only a portion of water actually seeping into the niche. In fact, evidence of the capillary barrier effect in this study was found in the sharp reduction in the wetting front travel velocity immediately above the niche, and also in the significant reduction in seepage rates as infiltration rates were reduced. The wetting front arrived at a fault location about 1 m above the ceiling (or 19 m below the infiltration plot) in 31 days, whereas seepage into niche 3 through the fault took place 35 days after the initial release of water. (Note that if a constant wetting front travel velocity is used, it took 1.6 days for the wetting front to travel 1 m.) Therefore water did not immediately seep into the niche after the wetting front arrived at the ceiling, an indication of the capillary barrier effect. Furthermore, Figure 7 suggests that the seepage recovery rate depends on the water release rate, with a lower release rate (after 16 February 2002) corresponding to a lower recovery rate. This may be caused by the capillary effect becoming stronger when capillary pressure in the fault and surrounding fractures is more negative (or as flow rate decreases).

4.2. Dynamic Flow Behavior

[34] Figure 6 shows the dynamic features of individual flow paths along the fault. A typical example is the flow path(s) associated with tray 6, within which there was a large degree of temporal variability in seepage rates. *Trautz and Wang* [2002] and *Dahan et al.* [1998] have also reported similar dynamic flow behavior in unsaturated fractures, which may result from a combination of mechanisms such as gravity-driven instabilities [*Nicholl et al.*, 1992, 1993a, 1993b, 1994], the development of capillary islands [*Su et al.*, 1999], or switches along fracture intersections [*Glass et al.*, 2002]. Additional mechanisms include alterations to the fault surface brought about by the shrinking/swelling of infill material within the fault [*Salve and Oldenburg*, 2001] and other alterations to fracture surfaces [e.g., *Weisbrod et al.*, 1998, 1999, 2000].

[35] While both laboratory and field observations [e.g., *Trautz and Wang*, 2002; *Dahan et al.*, 1998; *Su et al.*, 1999], including those in this study, consistently show the existence of dynamic flow behavior in unsaturated fractured rock at different scales, the temporal and spatial scales of the problem under consideration largely determine the practical importance of this dynamic behavior. For example, if our concern is the flow process for a given flow path, the dynamic behavior can be a dominant factor, one that needs to be considered (e.g., tray 6 in Figure 6). On the other hand, if we are mainly concerned with total seepage rate (as a function of time), the dynamic behavior may not be very important, because the relative temporal variability of the total seepage rate is considerably reduced. At the same time, we acknowledge that more theoretical and experimental studies are needed to fully understand the relative importance of the dynamic behavior at different scales.

4.3. Matrix Diffusion

[36] One major objective of this study was to evaluate the importance of matrix diffusion: it is considered to be a mechanism for retarding radionuclide transport through unsaturated fractured rock [*Bodvarsson et al.*, 2000]. This study differs from previous studies in that it involved multiple tracer transport and therefore allowed for a direct demonstration of the importance of matrix diffusion through unsaturated fractured rock. Compared with saturated systems [e.g., *Neretnieks*, 1980, 2002; *Moreno et al.*, 1997; *Jardine et al.*, 1999; *Shapiro*, 2001; *Reimus et al.*, 2003], the effects of matrix diffusion in unsaturated systems are more complex, owing to the multiphase flow processes

involved and the corresponding fracture-matrix interaction mechanisms.

[37] Several halide (bromide and iodide) and fluorobenzoic acid tracers have been used in unsaturated zone transport studies in the immediate vicinity of Yucca Mountain. At the Busted Butte site, located 8 km southeast of Yucca Mountain, these tracers were used to determine the extent of mixing/dispersion effects from several liquid injection episodes [*Turin et al.*, 2002]. In another study, *Reimus et al.* [2003] employed multiple tracers, including bromide and PFBA, in saturated borehole intervals drilled into the Bullfrog Tuff and Prow Pass Tuffs located approximately 2 km southeast of Yucca Mountain. In both tuff formations, a difference in the bromide and PFBA responses was observed, which the authors ascribed to matrix diffusion.

[38] Tracer test results from this study further support the importance of matrix diffusion. Figure 8 shows the bromide concentration of seeping water (collected at niche 3) as a function of time during early stages of the seepage tests. Because fractures and faults are probably initially dry and background bromide concentration is zero, the bromide concentration of seeping water would have been equal to the input concentration at the infiltration plot (25 mg/L), if there was no communication between fractures/faults and the neighboring matrix. Figure 8 shows a considerable degree of spreading in the breakthrough curve, indicating significant mixing of traced water with antecedent water in the matrix; matrix diffusion could be a significant contributor to this mixing process. In addition, Taylor dispersion and macrodispersion, caused by velocity variations within a rough-walled geometry (fractures and faults), could also contribute to the observed solute spreading, as discussed by *Detwiler et al.* [2000]. We can assess the magnitude of diffusion using a characteristic diffusion distance (L_{diff}) of $(D_{eff}\, t)^{0.5}$ [*Drever*, 1997]; the distance at which tracer relative concentration equals 0.5 is approximately 0.95 L_{diff}. As a first approximation we use the free water diffusion coefficient of bromide (2.15×10^{-10} m^2 s^{-1}) as the effective diffusion coefficient D_{eff} in the fault, and a travel time of 30 days for t. The diffusion distance thus obtained is 7.3 cm, which is much larger than the fault aperture of 1–2 cm observed at the alcove. Therefore Taylor dispersion caused by the velocity variations across the fracture aperture is probably negligible, and the observed dispersion of the breakthrough curve is related to matrix diffusion.

[39] The use of diffusivity tracers provides direct evidence of the importance of matrix diffusion, as shown in Figure 9. For breakthrough curves associated with tray 6, although a large degree of data fluctuation masks the concentration difference at early times (i.e., before 26 November 2001), the bromide concentrations along the descending breakthrough curves are considerably higher than PFBA concentrations, a signature of matrix diffusion. (A tracer with a larger molecular diffusion coefficient is subject to a larger degree of diffusion from matrix to the water in the fault (back diffusion), and therefore gives rise to larger concentration values.) The separation between breakthrough curves for two tracers is clearly indicated for tray 7 and tray 9 + 23. Before 24 December 2001, for a given time, the bromide generally corresponded to a smaller concentration value, because it has a larger molecular diffusion coefficient and is therefore subject to a larger degree of diffusion from the fault surface to the surrounding matrix. After 24 December 2001, the differences in concentration for the two tracers are not very well defined from the data points for tray 7. However, bromide concentrations are generally larger than those of PFBA from tray 9 + 23, which is consistent with the previous discussion regarding breakthrough curves for tray 6.

[40] The tracer breakthrough curves exhibit separation between bromide and PFBA, with PFBA arriving earlier than bromide in the arrival wave of the breakthrough curve (Figure 9). This is consistent with PFBA having a smaller aqueous diffusion coefficient than bromide, indicating the significance of matrix diffusion in controlling tracer transport in the field. Tracer transport is envisioned to be controlled by advective flow in fast flowing regions (faults and fractures), coupled with diffusive transfer among these regions into the neighboring tuff matrix. The separation between PFBA and bromide breakthrough curves (i.e., matrix diffusion contribution) is more evident in seepage water collected in tray 7, where seepage recovery was less than those in tray 6 and tray 9 + 23 (Figure 9). In the flow paths leading to liquid seepage in tray 7, advective flow through faults/fractures is probably slow (as suggested by the low seepage rates), which provides more time for matrix diffusion. The opposite is true for tray 6, where flow paths are more controlled by fault/fractures.

[41] Thus, while this experiment has provided preliminary insights on the nature of flow and transport at a relatively large temporal and spatial scale, it has also drawn attention to our limited understanding of how water moves through fractured rocks. Particularly, it has demonstrated the need to investigate mechanisms associated with capillary effects, and to investigate multiphase flow processes and corresponding fracture-matrix interactions influencing matrix diffusion.

[42] **Acknowledgments.** This work was supported by the Director, Office of Civilian Radioactive Waste Management, U.S. Department of Energy, through Memorandum Purchase Order EA9013MC5X between Bechtel SAIC Company, LLC and the Ernest Orlando Lawrence Berkeley National Laboratory (Berkeley Lab). The support is provided to Berkeley Lab through the U.S. Department of Energy contract DE-AC03-76SF00098. The efforts of Phil Rizzo were essential in fabrication of the equipment. Thanks to Diana Swantek for preparing illustrations and Irene Farnham for the chemical analysis of water samples. Thanks to Grace Su and Dan Hawkes for their careful review of this manuscript, and to two anonymous reviewers for their helpful comments and suggestions.

References

Albelin, H., L. Birgersson, J. Gidlund, and I. Neretnieks (1991), A large-scale flow and tracer experiment in granite: 1. Experimental design and flow distribution, *Water Resour. Res.*, *27*, 3107–3117.

Birkholzer, J., G. Li, C. F. Tsang, and Y. T. Tsang (1999), Modeling studies and analysis of seepage into drifts at Yucca Mountain, *J. Contam. Hydrol.*, *38*, 349–384.

Bodvarsson, G. S., W. Boyle, R. Patterson, and D. Williams (1999), Overview of scientific investigations at Yucca Mountain—The potential repository for high-level nuclear waste, *J. Contam. Hydrol.*, *38*, 3–24.

Bodvarsson, G. S., H. H. Liu, R. Ahlers, Y. S. Wu, and E. Sonnethal (2000), Parameterization and upscaling in modeling flow and transport at Yucca Mountain, in *Conceptual Models of Unsaturated Flow in Fractured Rocks*, Natl. Acad. Press, Washington, D. C.

Buesch, D. C., R. W. Spengler, T. C. Moyer, and J. K. Geslin (1996), Proposed stratigraphic nomenclature and macroscopic identification of lithostratigraphic units of the Paintbrush Group exposed at Yucca Mountain, Nevada., *U.S. Geol. Surv. Open File Rep.*, *94-469*.

Callahan, T. J., P. W. Reimus, R. S. Bowman, and M. J. Haga (2000), Using multiple experimental methods to determine fracture/matrix interactions and dispersion of nonreactive solutes in saturated volcanic tuff, *Water Resour. Res.*, *36*, 3547–3558.

Detwiler, R. L., H. Rajaram, and R. J. Glass (2000), Solute transport in variable-aperture fractures: An investigation of the relative importance of Taylor dispersion and macrodispersion, *Water Resour. Res.*, *36*, 1611–1625.

Dahan, O., R. Nativ, E. Adar, and B. Berkowitz (1998), A measurement system to determine water flux and solute transport through fractures in the unsaturated zone, *Ground Water*, *36*, 444–449.

Drever, J. I. (1997), *The Geochemistry of Natural Waters: Surface and Groundwater Environments*, 3rd ed., Prentice-Hall, Old Tappan, N. J.

Glass, R. J., M. J. Nicholl, S. E. Pringle, and T. R. Wood (2002), Unsaturated flow through a fracture-matrix network: Dynamic preferential pathways in mesoscale laboratory experiments, *Water Resour. Res.*, *38*(12), 1281, doi:10.1029/2001WR001002.

Hadermann, J., and W. Heer (1996), The Grimsel (Switzerland) migration experiment: Integrating field experiments, laboratory investigations and modeling, *J. Contam. Hydrol.*, *21*, 87–100.

Hu, Q., and J. S. Y. Wang (2003), Diffusion in unsaturated geological media: A review, *Crit. Rev. Environ. Sci. Technol.*, *33*, 275–297.

Hu, Q., R. Salve, W. Stringfellow, and J. S. Y. Wang (2001), Field tracer transport tests in unsaturated fractured tuff, *J. Contam. Hydrol.*, *51*, 1–12.

Jardine, P. M., W. E. Sanford, J. P. Gwo, O. C. Reedy, D. S. Hicks, J. S. Riggs, and W. B. Bailey (1999), Quantifying diffusive mass transfer in fractured shale bedrock, *Water Resour. Res.*, *35*, 2015–2030.

Lodman, D., S. Dunstan, W. Sowns, J. Sondrup, D. Miyasaki, K. Galloway, and K. Izbicki (1994), Treatability study report for the organic contamination in the vadose zone, *OU 7-08, Rep. EGG-ER-11121*, Idaho Natl. Eng. Lab., Idaho Falls.

Maloszewski, P., and A. Zuber (1993), Tracer experiments fractured rocks: Matrix diffusion and the validity of models, *Water Resour. Res.*, *29*, 2723–2735.

Meigs, L. C., and R. L. Beauheim (2001), Tracer tests in fractured dolomite: 1. Experimental design and observed tracer recoveries, *Water Resour. Res.*, *37*, 1113–1128.

Moreno, L., B. Gylling, and I. Neretnieks (1997), Solute transport in fractured media—The important mechanisms for performance assessment, *J. Contam. Hydrol.*, *25*, 283–298.

Native, R., E. Adar, O. Dahan, and M. Geyh (1995), Water recharge and solute transport through the vadose zone of fractured chalk under desert conditions, *Water Resour. Res.*, *31*, 253–261.

Neretnieks, I. (1980), Diffusion in the rock matrix: An important factor in radionuclide retardation?, *J. Geophys. Res.*, *85*, 4379–4397.

Neretnieks, I. (2002), A stochastic multi-channel model for solute transport-analysis of tracer tests in fractured rock, *J. Contam. Hydrol.*, *55*, 175–211.

Nicholl, M. J., R. J. Glass, and H. A. Nguyen (1992), Gravity-driven fingering in unsaturated fractures, in *Proceedings of the Third Annual International Conference on High Level Radioactive Waste Management*, pp. 321–331, Am. Nucl. Soc., La Grange Park, Ill.

Nicholl, M. J., R. J. Glass, and H. A. Nguyen (1993a), Small-scale behavior of single gravity-driven fingers in an initially dry fracture, in *Proceedings of the Fourth Annual International Conference on High Level Radioactive Waste Management*, pp. 2023–2032, Am. Nucl. Soc., La Grange Park, Ill.

Nicholl, M. J., R. J. Glass, and H. A. Nguyen (1993b), Wetting front instability in an initially wet unsaturated fracture, in *Proceedings of the Fourth Annual International Conference on High Level Radioactive Waste Management*, pp. 2061–2070, Am. Nucl. Soc., La Grange Park, Ill.

Nicholl, M. J., R. J. Glass, and S. W. Wheatcraft (1994), Gravity-driven infiltration instability in initially dry nonhorizontal fractures, *Water Resour. Res.*, *30*, 2533–2546.

Novalowski, K. S., and P. A. Lapcevic (1994), Field measurement of radial solute transport in fractured rock, *Water Resour. Res.*, *30*, 37–44.

Philip, J. R., J. H. Knight, and R. T. Waechter (1989), Unsaturated seepage and subterranean holes: Conspectus, and exclusion problem for cylindrical cavities, *Water Resour. Res.*, *25*, 16–28.

Reimus, P. W., M. J. Haga, A. L. Adams, T. J. Callahan, H. J. Turin, and D. A. Counce (2003), Testing and parameterizing a conceptual solute transport model in saturated fractured tuff using sorbing and nonsorbing tracers in cross-hole tracer tests, *J. Contam. Hydrol.*, *62–63*, 613–636.

Salve, R. (2004), A passive-discrete water sampler for monitoring seepage, *Ground Water*, in press.

Salve, R., and C. M. Oldenburg (2001), Water flow in a fault in altered nonwelded tuff, *Water Resources Res.*, *37*, 3043–3056.

Shapiro, A. M. (2001), Effective matrix diffusion in kilometer-scale transport in fractured crystalline rock, *Water Resour. Res.*, *37*, 507–522.

Su, G. W., J. T. Geller, K. Pruess, and F. Wen (1999), Experimental studies of water seepage and intermittent flow in unsaturated rough-walled fractures, *Water Resour. Res.*, *35*, 1019–1037.

Trautz, R. C., and J. S. Y. Wang (2002), Seepage into an underground opening constructed in unsaturated fractured rock under evaporative conditions, *Water Resour. Res.*, *38*(10), 1188, doi:10.1029/2001WR000690.

Turin, H. J., A. R. Groffman, L. E. Wolfsberg, J. L. Roach, and B. A. Strietelmeier (2002), Tracer and radionuclide sorption to vitric tuffs of Busted Butte, Nevada, *Appl. Geochem.*, *17*, 825–836.

Weisbrod, N., R. Nativ, D. Ronen, and E. A. Adar (1998), On the variability of fracture surfaces in unsaturated chalk, *Water Resour. Res.*, *34*, 1881–1887.

Weisbrod, N., R. Nativ, E. A. Adar, and D. Ronen (1999), Impact of intermittent flow of rainwater and wastewater on coated and uncoated fractures in chalk, *Water Resour. Res.*, *35*, 3211–3222.

Weisbrod, N., R. Nativ, E. A. Adar, D. Ronen, and A. Ben-Non (2000), The impact of coating and weathering the properties of chalk fracture surfaces, *J. Geophys. Res.*, *105*, 27,853–27,864.

Wood, W. W. (1996), Diffusion: The source of confusion?, *Ground Water*, *34*, 193.

P. Cook, A. Czarnomski, H.-H. Liu, and R. Salve, Earth Sciences Division, Lawrence Berkeley National Laboratory, Mail Stop 14-116, 1 Cyclotron Road, Berkeley, CA 94720, USA. (r_salve@lbl.gov)

Q. Hu, Lawrence Livermore National Laboratory, Livermore, CA 94550, USA.

D. Hudson, U.S. Geological Survey, MS 423, 1180 Town Center Drive, Las Vegas, NV 89144, USA.